LETTER

doi:10.1038/nature12002

July 2012 Greenland melt extent enhanced by low-level liquid clouds

R. Bennartz[1], M. D. Shupe[2], D. D. Turner[3], V. P. Walden[4], K. Steffen[2,5], C. J. Cox[4], M. S. Kulie[6], N. B. Miller[6] & C. Pettersen[6]

Melting of the world's major ice sheets can affect human and environmental conditions by contributing to sea-level rise. In July 2012, an historically rare period of extended surface melting was observed across almost the entire Greenland ice sheet[1,2], raising questions about the frequency and spatial extent of such events. Here we show that low-level clouds consisting of liquid water droplets ('liquid clouds'), via their radiative effects, played a key part in this melt event by increasing near-surface temperatures. We used a suite of surface-based observations[3], remote sensing data, and a surface energy-balance model. At the critical surface melt time, the clouds were optically thick enough and low enough to enhance the downwelling infrared flux at the surface. At the same time they were optically thin enough to allow sufficient solar radiation to penetrate through them and raise surface temperatures above the melting point. Outside this narrow range in cloud optical thickness, the radiative contribution to the surface energy budget would have been diminished, and the spatial extent of this melting event would have been smaller. We further show that these thin, low-level liquid clouds occur frequently, both over Greenland and across the Arctic, being present around 30–50 per cent of the time[3–6]. Our results may help to explain the difficulties that global climate models have in simulating the Arctic surface energy budget[7–9], particularly as models tend to under-predict the formation of optically thin liquid clouds at supercooled temperatures[6]—a process potentially necessary to account fully for temperature feedbacks in a warming Arctic climate.

Over the past few decades, the Arctic has experienced warming amplified by a set of positive feedbacks; these feedbacks include increased sea ice melt, increased atmospheric water vapour and cloudiness, and changes in atmospheric circulation patterns[10]. This warming has resulted in an increased extent of surface melt of the Greenland ice sheet (GIS) observed by satellite since 1979[11]. July 2012 set a new record in melt extent, with melting observed over nearly the entire GIS[1,2]. At Summit Station, a brief melting period was observed on 11 July 2012 (Fig. 1). Ice-core records from the same location indicate such events occur only about once every 150 yr (ref. 1) on average, with the last occurring in 1889[12]. The July 2012 melt event was triggered by advection of unusually warm air, with temperatures at 500 m above ground only slightly below freezing (Fig. 1). However, the observed surface melt at Summit cannot be explained by warm air advection alone, because the surface temperature over the GIS is controlled by a balance of radiative and turbulent heat fluxes[13–16] that are sensitive to cloud and atmospheric properties.

The local energy balance at the surface can be understood by accounting for three forcings on surface temperature, namely, the net radiative flux divergence at the surface, heat exchange with the atmosphere, and heat exchange with the underlying ice. A simple parametric model of these processes can be written as:

$$\frac{\partial T_S}{\partial t} = \underbrace{\frac{\alpha+1}{c_p \rho H}\Delta F_{NET}}_{\text{Radiative forcing}} + \underbrace{\frac{T_a - T_S}{\tau_a}}_{\text{Atmospheric heat exchange}} + \underbrace{\frac{T_i - T_S}{\tau_i}}_{\text{Ice heat exchange}} \quad (1)$$

This model is used here to study the effect of clouds on the temporal development of surface temperature. In equation (1), T_S is the surface temperature, t is time, H is the height of the inversion layer, α is a shape parameter characterizing the form of the temperature profile in the boundary layer, ρ is the average air density of the boundary layer, c_p is the specific heat of air, T_a is the temperature at the top of the inversion, T_i is the ice temperature at a depth low enough to be considered constant over the model integration time, ΔF_{NET} is the net radiative flux divergence at the surface, and τ_a and τ_i are relaxation timescales for heat exchange processes in the atmosphere and ice, respectively. Whereas the two heat exchange terms are non-negligible, the radiative forcing plays a dominant role in the development of surface temperature[14], which justifies the basic parameterizations of heat fluxes using relaxation times. In reality, atmospheric heat fluxes are complex functions of wind speed, turbulence state, temperature, and moisture profiles. The heat transfer into the surface depends on the snow's thermal conductivity but also on radiative heat exchange between different snow layers and solar radiation penetrating deeper into the snow layer[17]. The dependency of τ_a on atmospheric stability is simply modelled by making τ_a increase with increasing atmospheric stability, that is, $\tau_a = f(T_a - T_S)$. The model's response is not very sensitive to the choices of some of the model parameters; these parameters were fixed at $H = 210$ m, $\alpha = 2$, $\tau_i = 15$ h, and $T_i = -40\,^{\circ}$C. The particular choices of these parameters, as well as details of the model, are justified and outlined in the Supplementary Information.

The model assumes the temperature of the free atmosphere at the top of the inversion layer (T_a) to be a lateral boundary condition determined by advection. This temperature was determined from 12-hourly radiosonde observations at Summit. The individual radiative fluxes constituting ΔF_{NET}, the net radiative flux at the surface, are:

$$\Delta F_{NET} = F_{SW}^{\downarrow} - F_{SW}^{\uparrow} + F_{LW}^{\downarrow} - F_{LW}^{\uparrow} \quad (2)$$

The up and down arrows indicate the upwelling and downwelling radiation, respectively. The surface temperature model can be forced with observed or simulated radiative fluxes. Both approaches were performed for this study. For simulating fluxes, a simple atmospheric radiative transfer model was devised, which is outlined in the Supplementary Information. The shortwave component of the model $\left(F_{SW}^{\uparrow,\downarrow}\right)$ includes the radiative effects of water vapour, ozone, carbon dioxide, cloud liquid water, and surface albedo. The downwelling longwave component $\left(F_{LW}^{\downarrow}\right)$ accounts for thermal emission by atmospheric gases and cloud liquid water. The upwelling longwave radiation was simulated simply using Stefan–Boltzmann's law and a surface emissivity of unity, that is, $F_{LW}^{\uparrow} = \sigma_{SB} T_S^4$, where σ_{SB} is the Stefan–Boltzmann constant. The radiative transfer model does not account for ice clouds.

Figure 1a provides an overview of the temporal development of T_{2m}, the temperature at a height of two metres, both observed and simulated

[1]Atmospheric and Oceanic Sciences, University of Wisconsin, Madison, Wisconsin 53706, USA. [2]CIRES, University of Colorado and NOAA-ESRL, Boulder, Colorado 80305, USA. [3]NOAA–National Severe Storms Laboratory, Norman, Oklahoma 73072, USA. [4]Department of Geography, University of Idaho, Moscow, Idaho 83844, USA. [5]Swiss Federal Research Institute WSL, Birmensdorf, CH-8903, Switzerland. [6]Space Science and Engineering Center, University of Wisconsin, Madison, Wisconsin 53706, USA.

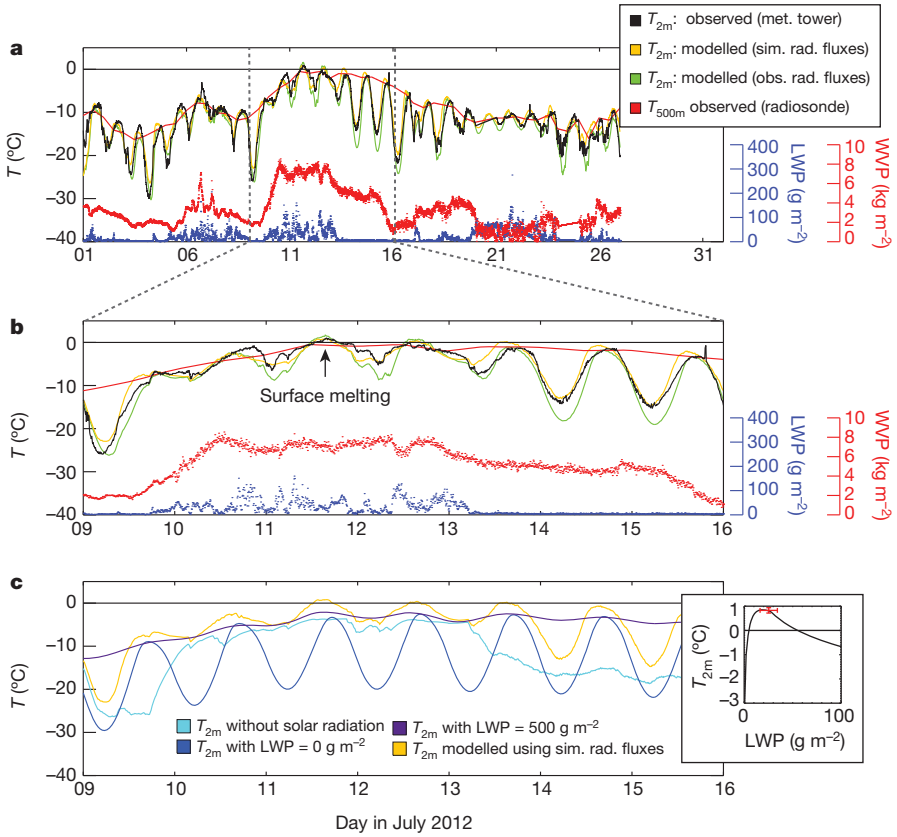

Figure 1 | Observed and simulated temporal evolution of the July 2012 surface melting event at Summit. **a**, Temporal evolution of the temperature 2 m above the surface (T_{2m}) for July 2012; **b**, expanded view of data from **a** for the extended GIS melting period (9–15 July 2012). In the top parts of **a** and **b**, the black curve shows T_{2m} observed by the NOAA meteorological (met.) tower, the red curve shows the temperature observed by radiosonde at 500 m above ground (T_{500m}), the green curve shows the development of T_{2m} simulated using the surface energy balance model driven by observed radiative (obs. rad.) fluxes[26], and the yellow curve shows the development of T_{2m} simulated using the surface energy balance model driven by simulated radiative (sim. rad.) fluxes based on water vapour path (WVP) and liquid water path (LWP). Values of these two last quantities are shown in the lower parts of **a** and **b** with separate axes: blue (red) dots show LWP (WVP) values observed by an upward looking microwave radiometer. **c**, Model sensitivity studies with respect to clouds and solar radiation. Yellow line, as in **a** and **b**; turquoise curve, T_{2m} without solar radiation; blue curve, T_{2m} assuming a cloud-free atmosphere (LWP = 0 g m^{-2}); purple curve, T_{2m} assuming an atmosphere with a very thick cloud with constant LWP of 500 g m^{-2}. Inset, simulated maximum T_{2m} (corresponding to the position of the arrow 'surface melting' in **b**) as a function of an assumed constant LWP; red data point shows the observed T_{2m} and LWP at a time of ±30 min around the time of maximum surface temperature (error bars, ±1 s.d.).

for July 2012 at Summit. For weaker surface inversions, this temperature will be very close to the surface temperature, $T_{2m} \approx T_S$. In the case of strong surface inversions, T_{2m} can be higher than T_S. Such cases might occur, for example, during the night under cloud-free conditions (for example, 14 July 2012). The cloud-free diurnal cycle of T_{2m} is of the order of 10 °C, with low temperatures during night caused by less incoming solar radiation and strong longwave energy loss. (We note that the solar zenith angle at the beginning of July at Summit is about 85° at local midnight and around 52° at local noon.) The surface melting period on 11 July 2012 was marked by low cloud bases, which occur very frequently over Summit. Low, liquid-bearing clouds were also present on 12 July 2012, followed by three cloud-free days. During the cloud-free period, and in particular on 13 July, warm air was still present over Summit but surface temperatures did not rise above 0 °C. A visual overview of cloudiness for July 2012 (as well as July 2010 and 2011 for comparison) is provided in Supplementary Fig. 5 and Supplementary Table 2, based on radar and lidar observations.

Despite its simplicity, the prognostic surface temperature model described in equation (1) reasonably captures the long-term variability, the phase and amplitude of the diurnal cycle, as well as its modulation by liquid clouds. Deviations occur in the presence of high ice clouds, which were not included in the simulations. Note that modelling results based on surface radiative flux observations agree well with the results where the surface radiative fluxes were computed using cloud observations and the radiative transfer model. This agreement confirms that ice clouds play a minor role in this particular study because the simulated radiative fluxes do not include effects of ice clouds whereas the observed fluxes do. The model also predicts the timing and strength of the surface melt event in July 2012 with reasonable accuracy (see Fig. 1b).

The modulating role of low-level liquid-containing clouds on the surface energy balance can be understood by considering two competing effects. First, these clouds reflect solar radiation to space, reducing shortwave energy available for surface warming and dampening the diurnal cycle. Second, low-level clouds radiate energy downwards in the infrared. This process is efficient even for very thin clouds. At liquid water path (LWP) values greater than 20 g m^{-2}, clouds become nearly completely opaque in the infrared[18,19] in which case the downwelling longwave radiation is determined almost entirely by cloud temperature. For the dry atmosphere observed over the GIS, cloudy-sky downwelling longwave fluxes can easily be 100 W m^{-2} higher than those measured for cloud-free conditions.

The relative balance of decreased solar radiation and increased downward longwave radiation depends on cloud optical properties, which are most strongly modulated by variations in LWP. Figure 1c shows model sensitivity studies for two extreme cases: no cloud (that is, LWP = 0 g m^{-2}) and an extremely thick cloud with LWP constant at 500 g m^{-2}. In the cloud-free case, a strong diurnal cycle exists but

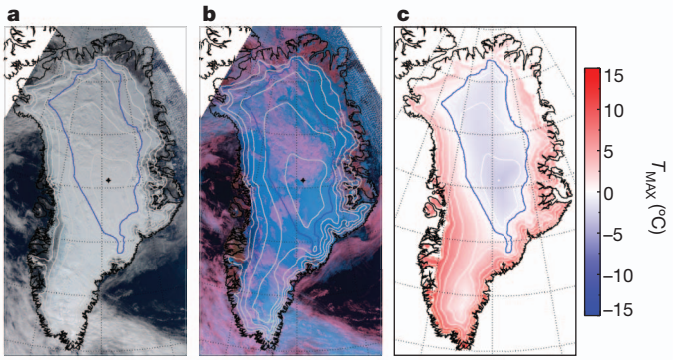

Figure 2 | Observed spatial distribution of clouds over Greenland on 11 July 2012 and their effect on surface temperature. **a**, Near-true-colour satellite image of Greenland observed by MODIS (on the Aqua satellite) on 11 July 2012, 14:55–15:05 UTC (MODIS channels 1, 4, 3). **b**, False-colour image for the same time period highlighting liquid-bearing clouds in purple (MODIS channels 7, 2, 1). The star shows the position of Summit. White contour lines give terrain height in 500-m intervals starting at 1,000 m. **c**, The maximum simulated temperature under cloud-free conditions (see text for details). The blue line corresponds to the 0 °C isothermal—that is, the height below which melting would occur under cloud-free conditions. This line is also shown in **a** and **b** as a reference.

near-surface temperatures do not rise above −4 °C. For the thick cloud, near-surface temperature follows the cloud temperature but does not exceed a value of −3 °C.

In neither of these two extreme cases does the near-surface temperature rise to values above the melting point. Only for a limited range of intermediate LWP values do the combined longwave and shortwave radiative effects conflate to push temperatures above 0 °C. Indeed, the energy balance model indicates that surface melting only occurs in this case for LWP values between 10 and 40 g m^{-2} (see Fig. 1c inset). Within this range, the cloud is opaque enough to 'trap' longwave radiation but still sufficiently thin to allow enough solar radiation to penetrate through to the surface. Clouds of this nature probably affected broad spatial areas of the GIS during this event. Figure 2a and b provide an overview of the cloud situation over the GIS on 11 July 2012, observed by the Moderate Resolution Imaging Spectrometer (MODIS) on NASA's Aqua satellite, and show extended liquid clouds over large parts of the central GIS.

Surface melting would not have occurred over Summit in July 2012 without the optically thin, liquid-water-containing clouds. However, temperatures were warm enough during this time to trigger melting without clouds at lower-elevation regions of the GIS. The diurnal cycle and the total amount of incoming solar radiation also vary with latitude. A second sensitivity study was carried out to estimate the relative impact of these two factors—that is, terrain height above sea level and latitude—on surface melting. Figure 2c shows the result of this sensitivity study, assuming cloud-free conditions and adjusting the model (equation (1)) for height effects on atmospheric temperature, downwelling longwave radiation, and incoming solar radiation as function of latitude. For all temperature dependencies on surface height, a climatological mean temperature lapse rate of 7.1 K km^{-1} was used[20]. Terrain slope and orientation were not considered, as terrain slopes on top of the GIS are generally small. This sensitivity study is not expected to reproduce the exact conditions observed over Greenland, but it does provide insight into the interplay of terrain height, available solar radiation, and clouds. The maximum simulated temperature (Fig. 2c) did not exceed 0 °C at terrain heights above roughly 2,700 m for regions south of Summit. At more northerly locations, where less solar radiation is available, these terrain heights fell below 2,000 m (see the blue 0 °C isothermal in all three panels of Fig. 2). In comparison, for a homogeneous cloud of 30 g m^{-2}, the model predicted melting everywhere (not shown). For this example model exercise, the spatial extent of GIS melt conditions increased from 61% to 100% as a result of the optically thin clouds.

This study highlights the intricate role of clouds in modulating the energy balance at the surface above the GIS in boreal summer. Thin, boundary-layer, liquid-containing clouds can change the surface energy balance towards warmer or colder surface temperatures depending on cloud optical thickness. In the case examined here, these clouds played a critical role in enhanced surface melt at Summit, Greenland, and probably contributed strongly to the 97% spatial melt extent observed over the GIS in early July 2012[1].

Thin, liquid-bearing clouds are ubiquitous across the Arctic[6]. Ground-based observations and model reanalysis products from the European Center for Medium Range Weather Forecasting (ERA-Interim) show occurrence frequencies ranging from 20% to more than

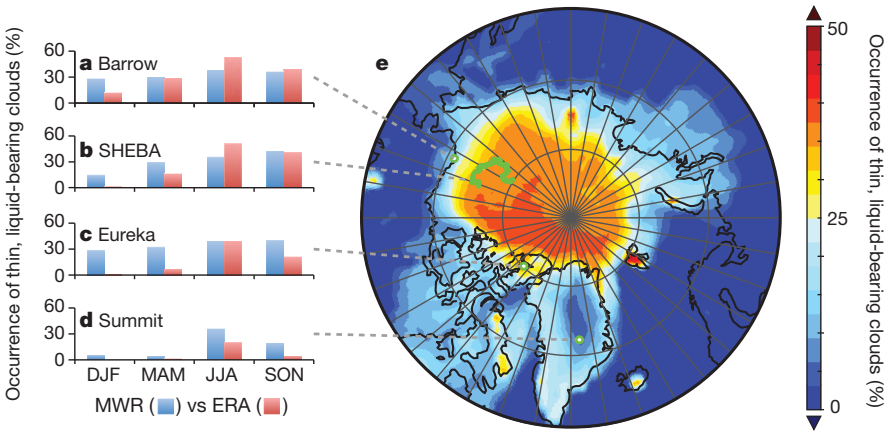

Figure 3 | Frequency of occurrence of thin, liquid-bearing clouds. For the purpose of this plot, 'thin, liquid-bearing' clouds are defined as clouds in the range of 10 g m^{-2} < LWP < 60 g m^{-2}, corresponding to the range of maximum enhanced cloud radiative forcing at the surface. **a**–**d**, Comparisons of ground-based observed (blue, microwave radiometer (MWR)) and ERA-Interim simulated (red, ERA) frequencies of occurrence of these clouds for four Arctic observation sites for all seasons; **a**, Barrow, Alaska; **b**, Surface Heat Budget of the Arctic Ocean (SHEBA) experiment (a research vessel frozen in the pack ice to study the ocean and atmosphere); **c**, Eureka, Nunavut (research base on Ellesmere Island, Canada); and **d**, Summit, Greenland. DJF, December–February; MAM, March–May; JJA, June–August; SON, September–November. **e**, Circumpolar map of the frequency of occurrence of these clouds from 32 yr of ERA reanalysis (1979–2011). The plot in **e** is conditionally sampled to only include cases with solar zenith angle lower than 80° and a surface albedo higher than 0.5; locations of the observation sites (**a**–**d**) are indicated.

50% of the time for four observational sites in summer and for most observational sites also in spring and autumn (Fig. 3a–d). (See Supplementary Information section 6 for details on the temporal coverage of the different observation sites; please also note that ERA-Interim histograms shown in Fig. 3a–d are restricted to the time period when observations are available.) Based on ERA-Interim reanalysis, Fig. 3e shows the occurrence of thin, liquid-bearing clouds in situations where the surface albedo is larger than 0.5 and at least some solar radiation is available (solar zenith angle less than 80°). These situations are most conducive to enhanced surface warming by the combined effects of solar and infrared warming discussed above[21–24]. Thin liquid clouds occur most frequently over sea-ice-covered areas north of 80° N, as well as over the Beaufort Sea and the east Siberian Sea, highlighting the importance of such clouds not only for the GIS but also for the surface energy balance over sea ice.

To simulate the surface energy balance correctly, it is imperative for climate models to accurately represent these liquid-containing clouds and their occurrence fraction, radiative properties and responses to a changing Arctic climate system. The comparisons provided in Fig. 3a–d highlight a significant shortcoming in our current modelling capabilities of Arctic clouds. ERA reanalysis provides mostly reasonable results for thin, liquid-cloud occurrence in summer months. However, the model significantly underestimates the occurrence of such clouds in winter and spring for most sites and for Summit in all seasons. A similar underestimation of the occurrence of thin, liquid clouds was recently reported[6] for global climate models based on comparisons with satellite-derived estimates of cloudiness. The discrepancies were attributed largely to the simplified treatment of cloud phase in models, which typically does not allow for liquid clouds to form at temperatures lower than about −20 °C. A similar phase determination scheme is employed in the ERA-Interim data, potentially explaining the significant low bias in modelled liquid-cloud occurrence over Summit (Fig. 3d). These shortcomings bias the Arctic surface energy balance predicted by present-day weather and climate models[6], and limit the ability of these models to predict the cloud response to Arctic climate change and possible feedbacks.

METHODS SUMMARY

Ground-based infrared, microwave, radar and lidar remote sensing observations, as well as radiosonde data, were collected as part of the project 'Integrated characterization of energy, clouds, atmospheric state, and precipitation at Summit' (ICECAPS)[3]. Cloud liquid-water path estimates were derived from multi-channel microwave measurements[4]. Downwelling longwave fluxes were derived from high-resolution infrared observations and cloud-free fluxes were calculated on the basis of radiosonde observations[25]. In addition, shortwave and longwave upwelling and downwelling radiative fluxes were observed from a suite of broadband radiometers[26,27], while temperatures at a height of two metres were observed from a meteorological tower operated by NOAA. All Summit, SHEBA, and Eureka ground-based data are available from the NOAA ESRL site (ftp://ftp1.esrl.noaa.gov/psd3/arctic/). Barrow data are available from the DOE ARM archive (http://www.archive.arm.gov/). MODIS satellite observations were obtained from NASA's Level 1 and Atmosphere Archive and Distribution System. ECMWF ERA Reanalysis data are available from the ECMWF data server (http://www.ecmwf.int).

Received 16 October 2012; accepted 8 February 2013.

1. Buis, A. & Cole, S. Satellites see unprecedented Greenland Ice Sheet melt. (NASA/JPL press release, 24 July 2012); available at http://www.jpl.nasa.gov/news/news.cfm?release=2012-217 (2012).
2. Nghiem, S. V. *et al.* The extreme melt across the Greenland Ice Sheet in 2012. *Geophys. Res. Lett.* **39,** L20502, http://dx.doi.org/10.1029/2012GL053611 (2012).
3. Shupe, M. D. *et al.* High and dry: new observations of tropospheric and cloud properties above the Greenland Ice Sheet. *Bull. Am. Meteorol. Soc.* **94,** 169–186 (2013).
4. Turner, D. D. *et al.* Retrieving liquid water path and precipitable water vapor from the atmospheric radiation measurement (ARM) microwave radiometers. *IEEE Trans. Geosci. Remote Sensing* **45,** 3680–3690 (2007).
5. Shupe, M. D. *et al.* Clouds at Arctic atmospheric observatories. Part I: occurrence and macrophysical properties. *J. Appl. Meteorol. Climatol.* **50,** 626–644 (2011).
6. Cesana, G., Kay, J. E., Chepfer, H., English, J. M. & de Boer, G. Ubiquitous low-level liquid-containing Arctic clouds: new observations and climate model constraints from CALIPSO-GOCCP. *Geophys. Res. Lett.* **39,** L20804, http://dx.doi.org/10.1029/2012GL053385 (2012).
7. de Boer, G. *et al.* A characterization of the present-day Arctic atmosphere in CCSM4. *J. Clim.* **25,** 2676–2695 (2012).
8. Klein, S. A. *et al.* Intercomparison of model simulations of mixed-phase clouds observed during the ARM mixed-phase Arctic cloud experiment. I: Single-layer cloud. *Q. J. R. Meteorol. Soc.* **135,** 979–1002 (2009).
9. Sandvik, A., Biryulina, M., Kvamsto, N. G., Stamnes, J. J. & Stamnes, K. Observed and simulated microphysical composition of arctic clouds: data properties and model validation. *J. Geophys. Res.* **112,** D05205, http://dx.doi.org/10.1029/2006JD007351 (2007).
10. Serreze, M. C. & Barry, R. G. Processes and impacts of Arctic amplification: A research synthesis. *Global Planet. Change* **77,** 85–96 (2011).
11. Mernild, S. H., Mote, T. & Liston, G. E. Greenland ice sheet surface melt extent and trends: 1960–2010. *J. Glaciol.* **57,** 621–628 (2011).
12. Clausen, H. B., Gundestrup, N. S., Johnson, S. J., Bindschadle, R. & Zwally, J. Glaciological investigations in the Crete area, central Greenland: a search for a new deep drilling site. *Ann. Glaciol.* **10,** 10–15 (1988).
13. Ohmura, A. Physical basis for the temperature-based melt-index method. *J. Appl. Meteorol.* **40,** 753–761 (2001).
14. Hudson, S. R. & Brandt, R. E. A look at the surface-based temperature inversion on the Antarctic plateau. *J. Clim.* **18,** 1673–1696 (2005).
15. Brandt, R. E. & Warren, S. G. Temperature measurements and heat transfer in near-surface snow at the South Pole. *J. Glaciol.* **43,** 339–351 (1997).
16. Bintanja, R. & van den Broeke, M. The influence of clouds on the radiation budget of ice and snow surfaces in Antarctica and Greenland in summer. *Int. J. Climatol.* **16,** 1281–1296 (1996).
17. Brandt, R. E. & Warren, S. G. Solar-heating rates and temperature profiles in Antarctic snow and ice. *J. Glaciol.* **39,** 99–110 (1993).
18. Turner, D. D. Improved ground-based liquid water path retrievals using a combined infrared and microwave approach. *J. Geophys. Res.* **112,** D15204, http://dx.doi.org/10.1029/2007JD008530 (2007).
19. Turner, D. D. *et al.* Thin liquid water clouds — their importance and our challenge. *Bull. Am. Meteorol. Soc.* **88,** 177–190 (2007).
20. Steffen, K. & Box, J. Surface climatology of the Greenland ice sheet: Greenland climate network 1995–1999. *J. Geophys. Res. D* **106,** 33951–33964 (2001).
21. Intrieri, J. M. *et al.* An annual cycle of Arctic surface cloud forcing at SHEBA. *J. Geophys. Res.* **107,** 8039, http://dx.doi.org/10.1029/2000JC000439 (2002).
22. Shupe, M. D. & Intrieri, J. M. Cloud radiative forcing of the Arctic surface: the influence of cloud properties, surface albedo, and solar zenith angle. *J. Clim.* **17,** 616–628 (2004).
23. Pavolonis, M. J. & Key, J. R. Antarctic cloud radiative forcing at the surface estimated from the AVHRR Polar Pathfinder and ISCCP D1 datasets, 1985–93. *J. Appl. Meteorol.* **42,** 827–840 (2003).
24. Persson, P. O. G. Onset and end of the summer melt season over sea ice: thermal structure and surface energy perspective from SHEBA. *Clim. Dyn.* **39,** 1349–1371 (2012).
25. Cox, C. J., Walden, V. P. & Rowe, P. M. A comparison of the atmospheric conditions at Eureka, Canada, and Barrow, Alaska (2006–2008). *J. Geophys. Res.* **117,** D12204, http://dx.doi.org/10.1029/2011JD017164 (2012).
26. Ohmura, A. *et al.* Baseline Surface Radiation Network (BSRN/WCRP): new precision radiometry for climate research. *Bull. Am. Meteorol. Soc.* **79,** 2115–2136 (1998).
27. Munneke, P. K. *et al.* The role of radiation penetration in the energy budget of the snowpack at Summit, Greenland. *Cryosphere* **3,** 277–306 (2009).

Supplementary Information is available in the online version of the paper.

Acknowledgements ICECAPS is supported by the US National Science Foundation (grants ARC-0904152, 0856773 and 0856559) as part of the Arctic Observing Network (AON) programme. Two-metre temperature and radar measurements were provided by the NOAA Earth System Research Laboratory. Lidar and ceilometer measurements were provided by the Department of Energy Atmospheric Radiation Measurement programme. We thank the extended ICECAPS team of scientists, engineers, students and field technicians for obtaining high-quality atmosphere and cloud observations at Summit.

Author Contributions R.B. conceived this study, developed the surface temperature model, and performed most of the data analysis; M.D.S. coordinated ICECAPS measurement streams and contributed to interpretation of cloud-surface interactions and Arctic cloud context; D.D.T. performed the physical retrievals to derive precipitable water vapour and liquid water path from the microwave radiometers, and analysed the cloud height distributions over Summit for the three July periods; V.P.W. served as Principal Investigator for the ICECAPS project, and oversaw the calculation of longwave downwelling clear-sky and all-sky fluxes; K.S. provided the broadband radiative flux observations; C.J.C. calculated longwave downwelling clear-sky fluxes from radiosonde observations and all-sky fluxes from spectrally highly resolving infrared observations; M.S.K. provided support developing multi-frequency microwave radiometer retrievals and retrieving/analysing operational datasets; N.B.M. provided ceilometer derived cloud fraction calculations and collected various operational datasets; and C.P. helped operate the radar, and helped identify the MODIS data and other observational datasets.

Author Information Reprints and permissions information is available at www.nature.com/reprints. The authors declare no competing financial interests. Readers are welcome to comment on the online version of the paper. Correspondence and requests for materials should be addressed to R.B. (bennartz@aos.wisc.edu).